

ACKNOWLEDGMENTS

This work is supported in part by the Office of

Naval Research, Metallurgy Program. The author wishes to thank Professor A. Miller and R. W. Kelly for reading over this manuscript.

¹M. H. Rice, R. G. McQueen, and J. M. Walsh, in *Solid State Physics*, edited by F. Seitz and D. Turnbull (Academic, New York, 1958), Vol. 6, p. 1.

²P. P. Gillis and J. Kratochuil, *Phil. Mag.* **21**, 425 (1970).

³A. H. Cottrell, *Dislocation and Plastic Flow in Crystals* (Oxford U.P., Oxford, England, 1956), p. 42.

⁴J. Weertman, in *Response of Metals to High Velocity Deformation*, edited by P. G. Shewmon and V. F. Zackay (Interscience, New York, 1960), p. 205.

⁵W. G. Johnson and J. J. Gilman, *J. Appl. Phys.* **30**,

129 (1959).

⁶C. K. Dharan Hari, Lawrence Radiation Laboratory Report No. UCRL-18549, 1968 (unpublished).

⁷J. J. Gilman, *Micromechanics of Flow in Solids* (McGraw-Hill, New York, 1969), p. 219.

⁸J. W. Taylor, *J. Appl. Phys.* **36**, 3148 (1965).

⁹G. R. Cowan, *Trans. Met. Soc. AIME* **233**, 1120 (1965).

¹⁰P. Beardmore, A. H. Holtzman, and M. B. Bever, *Trans. Met. Soc. AIME* **230**, 725 (1964).

PHYSICAL REVIEW B

VOLUME 5, NUMBER 8

15 APRIL 1972

Optical Properties of Single-Crystal Zinc[†]

J. H. Weaver, D. W. Lynch, and R. Rosei*

Department of Physics and Institute for Atomic Research, Iowa State University, Ames, Iowa 50010
(Received 9 December 1971)

Measurements were made of the absorptivity of single crystals of zinc from 0.1 to 3.0 eV at 4.2 K. Polarized radiation was used with the electric field vector parallel or perpendicular to the c axis of the crystal. New structure was found for $\vec{E} \parallel \hat{c}$ at about 0.15 eV; no low-energy structure was observed for $\vec{E} \perp \hat{c}$. The low-energy interband transition is attributed to transitions near the point K in the Brillouin zone. The structure in the near-infrared and visible spectra is highly temperature dependent. Comparisons of the absorptivity and the conductivity are made between our 4.2-K data and the data of Rubloff for 77 and 300 K and with the calculations of Kasowski. Thermomodulation measurements on basal-plane samples are described which show the conductivity doublet as originating from two distinct infrared-absorption structures. The low-energy absorptivity is found to be nearly constant for $\vec{E} \parallel \hat{c}$. An optical effective-mass component m_{if}^* of $2.0m_0$ is computed from theories of the anomalous skin effect.

INTRODUCTION

Recently, the optical properties of Zn have been the subject of both experimental¹⁻⁴ and theoretical⁵ investigations. Reflectivity measurements have been performed by Rubloff from 0.6 to 4.0 eV at 300 and 77 K,¹ and by Mosteller and Wooten from 2.2 to 10.8 eV at 96 K.² Rubloff measured the spectrum with \vec{E} parallel and perpendicular to the c axis of the crystal. His crystals were mechanically polished, electropolished, and then transferred to a vacuum chamber. He found that the effect of ZnO was significant at energies greater than about 3.0 eV. Mosteller and Wooten were able to eliminate the oxide problem by cleaving their crystals in an ultra-high-vacuum chamber and performing their measurements *in situ*; of course, in this way they were able to investigate only basal-plane samples.

Calculations of the band structure of Zn have been performed by Stark and Falicov.⁶ A strongly non-local pseudopotential model⁷ was used and the

pseudopotential Fourier coefficients were adjusted to fit existing Fermi-surface data. Kasowski⁵ used the band structure of Stark and Falicov to calculate the interband optical spectra. A detailed comparison of Kasowski's predictions with experimental data has been presented by Rubloff.¹

The low-energy limit of data on Zn has previously been 0.6 eV, while Kasowski has predicted structure in the conductivity at energies somewhat below 0.4 eV. Accordingly, we felt it worthwhile to investigate the low-energy region, particularly because interband transitions had been found in Cd at about 0.29 eV.⁸ Furthermore, optical measurements had never been performed on Zn at 4.2 K. In the following we present our low-energy, low-temperature data. We show that there is indeed a low-energy interband transition for $\vec{E} \perp \hat{c}$. Our data extend to 3.0 eV and indicate that there is a considerable temperature shift of the optical spectrum upon cooling from 77 to 4.2 K—a greater shift, in fact, than occurs between 300 and 77 K. We also present thermoreflexion measurements,

made to search for structure in the interband dielectric constant that may be hidden. No new structure was found.

EXPERIMENTAL METHOD

Our measurements were of two kinds, absorptivity and thermomodulation. For the absorptivity measurements, oriented single crystals of zinc were studied by a calorimetric technique.⁹ The samples had measured residual-resistivity ratios of about 1250 for both $\vec{E} \perp \hat{c}$ and $\vec{E} \parallel \hat{c}$ and had an estimated purity of 99.999%.¹⁰ Samples initially were prepared by spark cutting and mechanical polishing, but such an approach produced slip bands which were evident on the sample faces. While the surfaces appeared to be flat, it was impossible to estimate the effect of the slip bands on the measured absorptivity. Consequently, an acid saw was used to cut the samples to the desired size (about 9×12 mm). This technique proved to be satisfactory and no slip bands were observed. The samples were polished with an acid polisher thereby eliminating straining and work damaging the surface. The resulting sample surfaces were somewhat wavy, but our gold-black absorber was sufficiently large to collect all but a very small fraction of any nonspecularly reflected light. Since the polishing process necessarily took place as much as an hour before the sample could be mounted, a chemical etch was used to remove the ZnO layer from the surface. A solution of $\text{CrO}_3 : \text{NaSO}_4 : \text{H}_2\text{O}$ (200 : 15 : 100) was used, followed by a solution of equal parts of HNO_3 , H_2O_2 , and H_2O . An equally satisfactory final etch was dilute HNO_3 . In either case, the sample was rinsed in methanol, dried in a nitrogen stream, mounted in the calorimeter chamber, and the chamber was evacuated. An average time of 15 min elapsed before the chamber was at 10^{-4} Torr; within

3 h the sample was at 77 K and liquid helium was transferred.

Our second type of measurement was of thermomodulation.^{11,12} Samples were prepared by standard techniques in a vacuum of $(1-5) \times 10^{-8}$ Torr. Two approaches were used. In one, the substrate was cooled to near 77 K and zinc was deposited from a Mo boat directly onto the substrate. In the second, a very thin film of nickel was deposited prior to the deposition of the zinc onto the 300-K substrate. Both methods were satisfactory for our $\Delta R/R$ measurements. Once a sample was prepared, it was removed from the vacuum chamber, mounted on a sample holder, and the chamber was evacuated to 10^{-6} Torr, all within about 30 min. Within an hour, the sample was cooled to 77 K.

Our absorptivity (A) data were obtained by a calorimetric technique. The relative accuracy in A is estimated to be 2% at 2 eV, but only about 5% at 0.1 eV. Sensitivity for structure in A is estimated to be 0.001. A AgCl pile-of-plate polarizer was used with a globar source for photon energies less than about 0.7 eV; a Glan prism was used for higher energies.

The thermomodulation measurements were performed in a manner discussed elsewhere.¹² All measurements were made at about 120 K. When the modulation samples were prepared, an identical film was simultaneously prepared and used for calorimetric measurements of A . The spectra of A showed the samples to have the c axis perpendicular to the sample face ($\vec{E} \perp \hat{c}$) with no evidence of the structure characterizing the parallel polarization. Accordingly, the thermomodulation data presented here are for $\vec{E} \perp \hat{c}$ only.

RESULTS

Figure 1 shows the absorptivity of zinc at 4.2 K

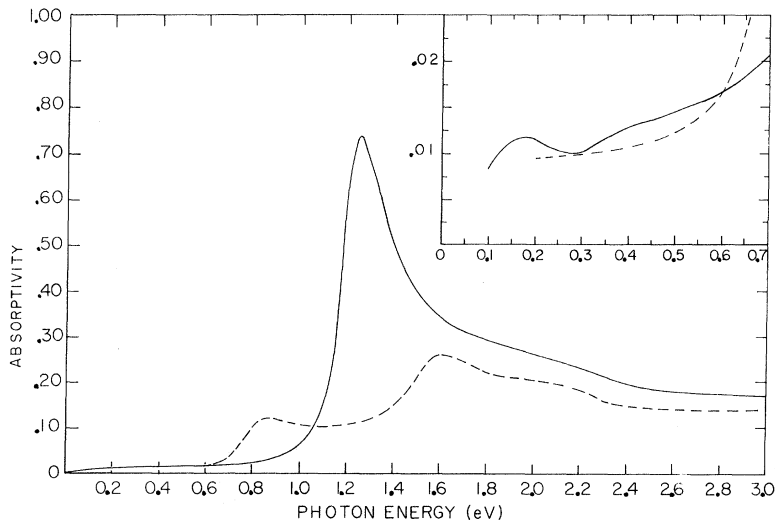


FIG. 1. Absorptivity of Zn at 4.2 K, 15° angle of incidence. The insert shows the low-photon-energy region. Solid line, $\vec{E} \perp \hat{c}$; dashed line, $\vec{E} \parallel \hat{c}$.

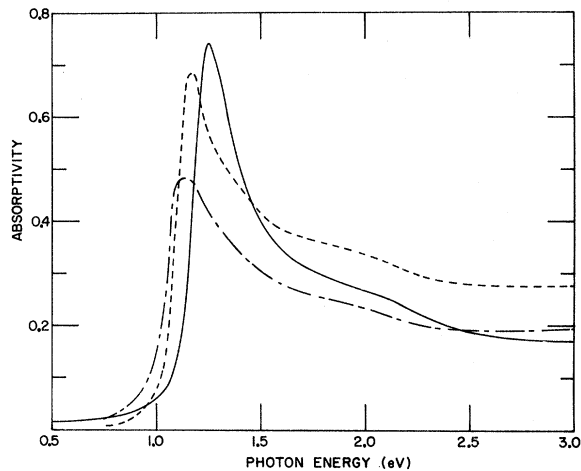


FIG. 2. Absorptivity of Zn for $\vec{E} \perp \hat{c}$ at three temperatures. Solid line, present work at 4.2 K; dashed line data of Ref. 1 at 77 K; dot-dashed line, data of Ref. 1 at 300 K.

for both $\vec{E} \perp \hat{c}$ and $\vec{E} \parallel \hat{c}$. The insert shows the low-energy absorptivity. The $\vec{E} \perp \hat{c}$ data were obtained using polarized light and samples with the c axis in the surface plane; the data were extended farther into the infrared by using a basal-plane sample and unpolarized light. The effective low-energy limit was 0.2 eV for polarized light and 0.1 eV for unpolarized light. Structure near 0.15 eV with $\vec{E} \perp \hat{c}$ is presented for the first time, as is a very small structure at about 0.4 eV. A qualitative comparison of the present Zn data with previously published Cd data⁸ brings out the following features:

(a) The $\vec{E} \perp \hat{c}$ spectra are quite similar in appearance. Both display a large sharp peak followed by a shoulder on the high-energy side of the peak.

While for Cd the peak was near 1.0 eV, we have found the Zn peak to be at 1.225 eV (at 4.2 K). Further, the shoulder appears to be smaller in Zn and is evident at about 0.3-eV higher energy.

(b) The structure near 0.15 eV for $\vec{E} \perp \hat{c}$ is seen to correspond to the structure observed in Cd at 0.29 eV. In neither Zn nor Cd is there any observed low-energy structure for $\vec{E} \parallel \hat{c}$.

(c) In Cd there is weak structure at 0.8 eV in the $\vec{E} \parallel \hat{c}$ spectrum. In Zn, the structure is considerably more prominent and is centered at roughly the same energy.

(d) The Zn spectrum shows two broad structures in A for $\vec{E} \parallel \hat{c}$ with the maxima occurring at roughly 1.6 and 2.1 eV. For Cd there was only the single sharp peak at 1.1 eV.

In Fig. 2 we compare our Zn data for $\vec{E} \perp \hat{c}$ with those of Rubloff,¹ who measured the reflectivity at 77 and 300 K. The temperature dependence of the structure is clearly evident. The large peak sharpens and shifts from 1.225 to 1.175 to 1.15 eV as the temperature changes from 4.2 to 77 to 300 K.

The maximum of the shoulder at about 2.0 eV is somewhat harder to define, but the shoulder appears to shift toward higher energy as the temperature is reduced. The magnitude of the 77-K data is probably too large at energies above about 1.4 eV as was pointed out by Rubloff. The good agreement of our 4.2-K data with the 300-K data suggests that indeed the absorption above 1.4 eV at 77 K is erroneously high.

The temperature dependence of A for $\vec{E} \parallel \hat{c}$ is shown in Fig. 3. The peak at 1.6 eV is seen to shift to about 1.5 eV and then to 1.45 eV as the temperature is varied from 4.2 to 77 to 300 K. It appears that the shoulder at about 2.1 eV also shifts toward higher energy with reduced temperature, but again the maxima are less clearly defined. It is also apparent that the low-energy peak at 0.8 eV is somewhat anomalous in that the shift of the peak energy is in the direction opposite to the other shifts: As the temperature is reduced, the peak shifts to lower energy. Note that for this polarization the three sets of data are in excellent agreement near 3.0 eV.

The data have been analyzed using a standard Kramers-Kronig (KK) technique to calculate the phase angle. The optical constants were then calculated. Since ZnO absorbs strongly above 3.34 eV,¹³ extrapolations to join our 3.0-eV data smoothly to those of Mosteller and Wooten² were performed. We feel a smooth matching is possible since the absorptivity between roughly 3 and 7 eV is flat.² The behavior in the infrared beyond the range of our data was assumed to be of a Drude nature and the curves were extrapolated smoothly to zero energy.

Our conductivity data for $\vec{E} \perp \hat{c}$ and $\vec{E} \parallel \hat{c}$ are presented in Figs. 4 and 5, respectively. Also shown are the data presented by Rubloff for 77 and 300 K. The histogram represents the interband conductivity calculated by Kasowski.⁵ Our data are in good

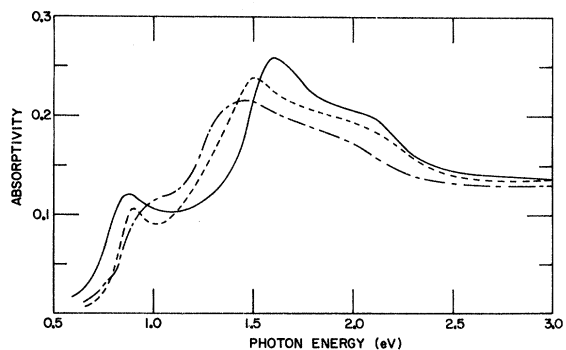


FIG. 3. Absorptivity of Zn for $\vec{E} \parallel \hat{c}$ at three temperatures. Solid line, present work at 4.2 K; dashed line, data of Ref. 1 at 77 K; dot-dashed line, data of Ref. 1 at 300 K.

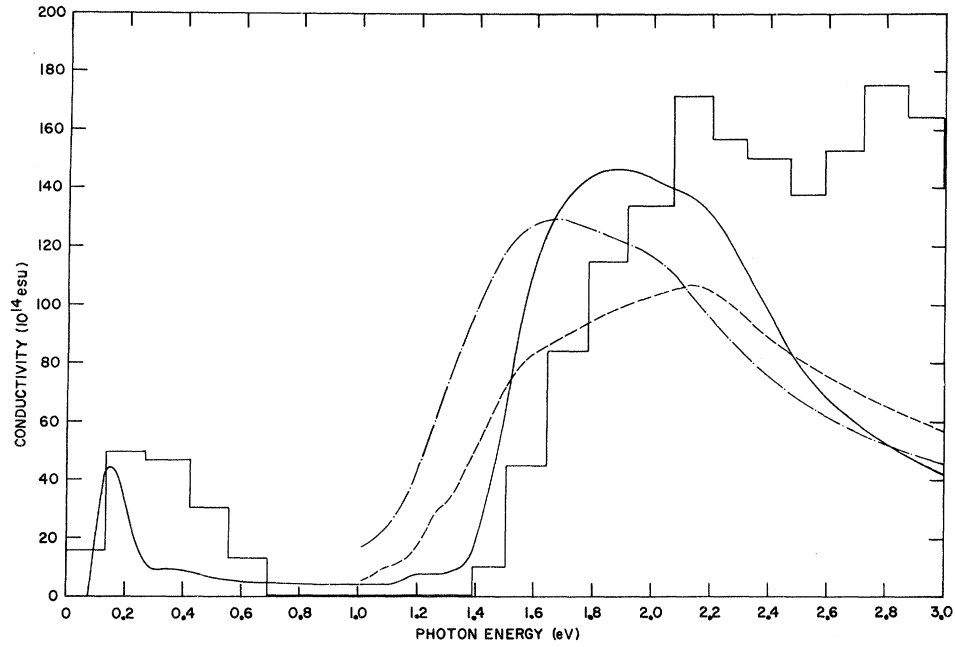


FIG. 4. Optical conductivity for $\vec{E} \perp \hat{c}$. The histogram represents the calculated spectrum at 0 K of Ref. 5, while the 77 (dashed) and 300 K (dot-dashed) curves represent the work of Ref. 1. The solid line is the present work at 4 K.

agreement with those of Rubloff and show clearly the temperature effect on the spectrum.

The partial sum rule giving $N_{\text{eff}}(E)$, the number of electrons per atom contributing to absorption below energy E , was evaluated with our ϵ_2 data.

Between 0.1 and 3.0 eV, N_{eff} was 1.2 electrons/atom for $\vec{E} \perp \hat{c}$ and 1.1 electrons/atom for $\vec{E} \parallel \hat{c}$ from interband transitions alone. The free-electron contribution between 0 and 0.1 eV is difficult to evaluate, except at low temperature, where $E\tau/$

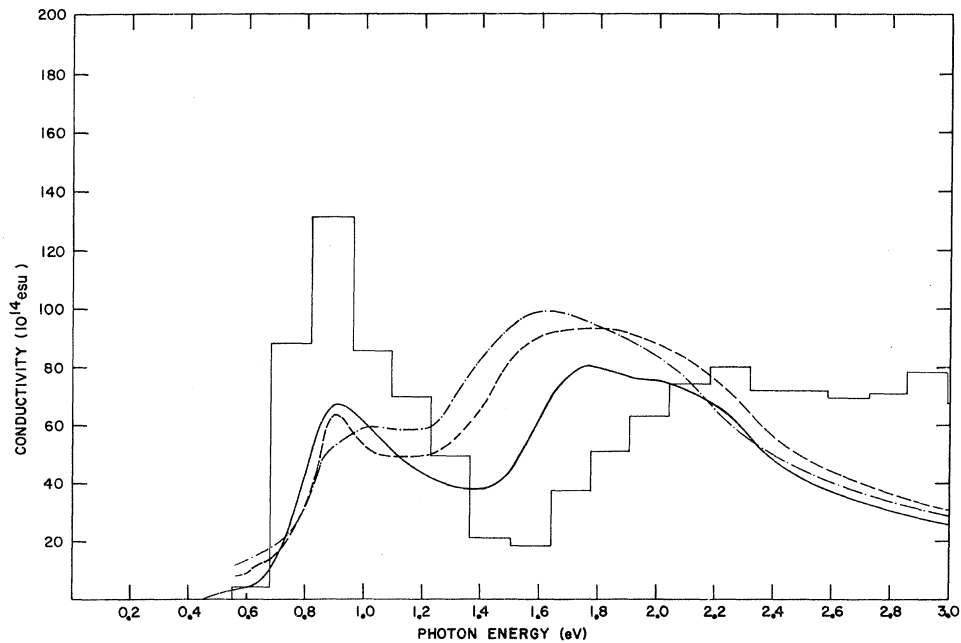


FIG. 5. Optical conductivity for $\vec{E} \parallel \hat{c}$. The histogram represents the calculated spectrum at 0 K of Ref. 5, while the 77 (dashed) and 300 K (dot-dashed) curves represent the work of Ref. 1. The solid line is the present work at 4 K.

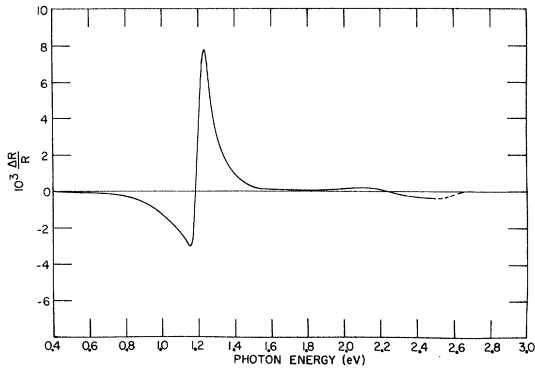


FIG. 6. Thermorefectivity spectrum ($\Delta R/R$) of Zn at about 120 K; input power about 2.4 W. The dashed curve beyond 2.5 eV represents a guess at the behavior of $\Delta R/R$.

$\hbar \gg 1$. Then $N_{\text{eff}}(E) \approx 2.0/m^* \approx 1$ electron/atom.

Figure 6 presents the thermorefectance spectrum, i.e., the normalized temperature shift of the reflectivity $\Delta R/R$ in the energy range from 0.5 to 2.5 eV taken at about 120 K. Two structures are clearly visible, one arising from the modulation of the strong peak at about 1.2 eV and the other from the shoulder at about 2.2 eV. We see that the points where the curve crosses the axis correspond very well to the peak energies for the absorptivity measured by Rubloff at 77 K. In fact, Fig. 6 resembles the negative of the derivative of the dashed curve in Fig. 2. We present no KK analysis of our $\Delta R/R$ spectrum since to do so would require very accurate spectra of ϵ_1 and ϵ_2 for $\vec{E} \perp \hat{c}$ at about 120 K; such data are not available. Reliable data were, of course, on hand for 300 and 4.2 K, but while the spectrum of σ and thus ϵ_2 at about 120 K can be assumed to lie between the 300- and 4.2-K curves of Fig. 4, an accurate curve cannot be drawn. KK analysis using "interpolated" spectra of $\bar{\epsilon}$ proved to be very sensitive to small changes in $\bar{\epsilon}$. Hence KK analysis of our $\Delta R/R$ spectrum cannot be done reliably at present.

DISCUSSION

Stark and Falicov⁶ calculated the band structure shown in Fig. 7 using a nonlocal pseudopotential model; Kasowski⁵ calculated the interband conductivity (σ_i) spectrum based upon these band calculations, neglecting spin-orbit coupling. His spectra for σ_i at 0 K are represented by the histograms in Figs. 4 and 5. To compare the present experimental conductivity with theory, we calculated a Drude-like conductivity, using our infrared data.¹⁴ We then subtracted the free-electron contribution; our 4.2-K conductivity curve represents only the interband conductivity σ_i . Since the data presented by Rubloff combined interband and intraband effects, we reproduce his curves only for photon energies greater than about 1.0 eV, where the free-electron contribution is small.

Comparison of the low-energy data shows good agreement of theory with experiment. Strong structure is clearly evident at about 0.15 eV. Also evident, but on less firm ground, is a hump at about 0.40 eV corresponding to the small shoulder in A at about 0.40 eV. The doublet structure calculated by Kasowski is experimentally observed, though the center of the calculated structure occurs about 0.7 eV too high. We also find that while the magnitude of the theoretical structure agrees reasonably well with the experimental curves, the resolution in the doublet is quite exaggerated in the theoretical representation.

To investigate further the origin of the doublet, the thermomodulation experiments were performed. From Fig. 6 we see only two reflectance structures in the energy range 0.5–2.5 eV. We believe that the doublet is made of two contributions, weighted by the KK analysis, the large A peak at 1.225 eV and the shoulder at 2.2 eV. If the shoulder in A at about 2.2 eV is smoothed out, the conductivity displays only a single peak.

The temperature dependence of the interband transitions for $\vec{E} \perp \hat{c}$ is clearly seen in Fig. 4. As

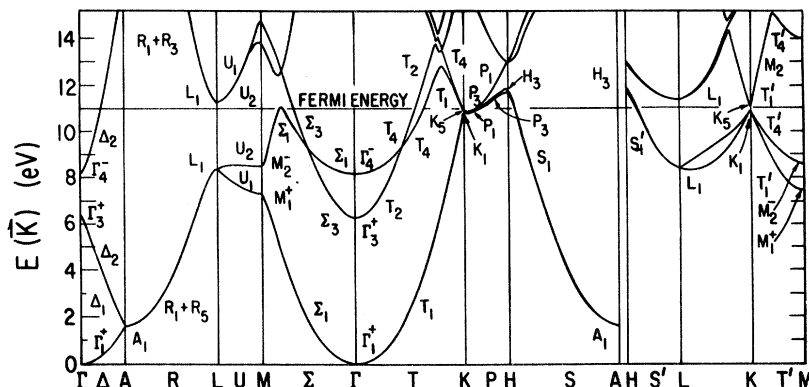


FIG. 7. Band structure of Zn from Ref. 6.

the temperature is increased, the structure shifts toward lower energy. This is probably a result of the phonon weakening of the crystal potential as discussed by Kasowski and Rubloff. It should be pointed out that the temperature shift appears to be greater in the 0–77-K range than for the range 77–300 K. This is true for both polarizations.

In Fig. 5 we show the conductivities for $\vec{E} \parallel \hat{c}$. We again find a difference of about 0.7 eV between our data and the calculated doublet center. The doublet is more clearly defined in our spectrum than in previous work, probably because the absorptivity shoulders are sharper at 4.2 K. The spectrum again appears to shift toward higher energies with reduced temperature. The temperature dependence observed in the A structure at 0.8 eV is apparently lost in KK analysis since we see no temperature shift for the 0.9-eV conductivity structure.

The observed interband transitions are probably well explained by Kasowski. He attributes the doublet structure in both polarizations to transitions along LH (see Fig. 7). The large anisotropic peak occurring with $\vec{E} \parallel \hat{c}$ at 0.9 eV is attributed to transitions along ΓM and ΓK ; these are electric-dipole-forbidden transitions for $\vec{E} \perp \hat{c}$. We attribute the new structure observed for $\vec{E} \perp \hat{c}$ at about 0.15 eV to transitions near K . The calculated low-energy structure is broader and is centered at a higher energy than the observed structure. The discrepancy probably arises from "noise" in the calculations of low-energy structure. The temperature dependence of the structure has been explained in some detail by both Kasowski and Rubloff. We note that little light can be shed on the anomalous temperature dependence mentioned by Rubloff for the $\vec{E} \parallel \hat{c}$ structure at 0.9 eV since no shift of that structure was observed.

Free-Electron Region

Our absorptivity data extend to 0.2 eV for $\vec{E} \parallel \hat{c}$ and to 0.1 eV for $\vec{E} \perp \hat{c}$. Since a low-energy interband transition has been found for $\vec{E} \perp \hat{c}$, but not for $\vec{E} \parallel \hat{c}$, we can discuss conduction-electron absorption processes only for $\vec{E} \parallel \hat{c}$.

For sufficiently pure metals at 4.2 K, the Drude model is not sufficient to explain the intraband absorption of radiation. The electron mean free path is no longer small compared to the skin depth, and a nonlocal expression relating the electric fields to the current density must be considered. This is the anomalous skin effect. Reuter and Sondheimer¹⁵

presented a theory taking into account surface scattering of an electron emerging from the interior of the metal. They predicted an absorptivity of $A = \frac{3}{4}(v_F/c)$, where v_F is the Fermi velocity and diffuse scattering of electrons at the surface is assumed. Bulk-scattering processes within the skin depth were considered by Holstein¹⁶ and the total absorption was calculated to be

$$A = \frac{3v_F}{4c} + \frac{2}{\omega_p \tau'} + \frac{2}{\omega_p \tau} \frac{2\Theta}{5T}, \quad (1)$$

where Θ is the Debye temperature, ω_p is the free-electron plasma frequency, τ is the relaxation time as determined by dc resistivity measurements at $T > \Theta$, and τ' is the relaxation time at the temperature at which A is measured. A relaxation time for the bulk electron-phonon scattering can be identified as $\frac{5}{2}(T/\Theta)\tau$. Fuchs and Kliewer¹⁷ generalized Eq. (1) to include non-normal incidence and found

$$A = 2\gamma \cos\phi \left[1 - \frac{1}{8}(\gamma/\Omega)^2 + \frac{1}{2}\Omega^2 \cos^2\phi - \gamma \cos\phi \right] + \frac{3}{4}(v_F/c) \cos\phi \left[1 - (\gamma/\Omega)^2 - 2\gamma \cos\phi \right] - (v_F/c)^2 \cos\phi \left[\frac{65}{128}(\gamma/\Omega)^2 + \frac{9}{32} \cos\phi \right], \quad (2)$$

where ϕ is the angle of incidence, $\Omega = \omega/\omega_p$, and

$$\gamma = 1/\omega_p \tau' + (1/\omega_p \tau)^{\frac{2}{5}} \Theta/T.$$

From Fig. 1 we find the magnitude of A is 0.0093 at 0.2 eV for $\vec{E} \parallel \hat{c}$. If we use a free-electron value for the Fermi velocity, we find $\frac{3}{4}v_F/c = 0.00456$. Since our measured resistivity ratios were about 1250, we can neglect the scattering term $1/\omega_p \tau'$. Using the values $\Theta = 310$ K, $\hbar\omega_p = 13.41$ eV, and $\sigma_{||} = 1.48 \times 10^{17}$ esu,¹⁸ we calculate the values of the absorptivity to be 0.0145 and 0.0133 from Eqs. (1) and (2), respectively. If we force a fit⁹ between Eq. (1) and the experimental absorptivity by adjusting m^* and τ to give both $\sigma_{||}$ and the low-temperature absorptivity, we find $m_{||}^* = 2.0m_0$. A similar fit using Eq. (2) gives $m_{||}^* = 1.8m_0$. We cannot perform similar calculations to obtain m_{\perp}^* . The thermal effective mass is $2.02m_0$.¹⁹ Agreement is surprisingly good since phonon-mass enhancement is expected to make m_{thermal}^* larger than m_{optical}^* by less than 12%.²⁰

ACKNOWLEDGMENTS

The authors thank M. Murtha for providing the zinc crystals and for his help with the acid saw and acid polisher. We also acknowledge the helpful suggestions of G. W. Rubloff and K. L. Kliewer.

[†]Work performed in the Ames Laboratory of the U. S. Atomic Energy Commission. Contribution No. 3166.

*Present address: Istituto di Fisica dell'Università, Rome, Italy.

¹G. W. Rubloff, Phys. Rev. B **3**, 285 (1971).

²L. P. Mosteller and F. Wooten, Phys. Rev. **171**,

743 (1968).

³A. H. Lettington, in *Optical Properties and Electron Structures of Metals and Alloys*, edited by F. Abeles (North-Holland, Amsterdam, 1966).

⁴R. H. W. Graves and A. P. Lenham, J. Opt. Soc. Am. **58**, 126 (1968).

- ⁵R. V. Kasowski, Phys. Rev. **187**, 885 (1969).
⁶R. W. Stark and L. M. Falicov, Phys. Rev. Letters **19**, 795 (1967).
⁷W. A. Harrison, *Pseudopotentials in the Theory of Metals* (Benjamin, New York, 1966).
⁸R. J. Bartlett, D. W. Lynch, and R. Rosei, Phys. Rev. B **3**, 4074 (1971).
⁹L. W. Bos and D. W. Lynch, Phys. Rev. B **2**, 4567 (1970).
¹⁰M. Murtha (private communication).
¹¹M. Cardona, *Modulation Spectroscopy* (Academic, New York, 1969).
¹²R. Rosei and D. W. Lynch (unpublished).
¹³R. L. Hengehold and R. J. Almassy, Phys. Rev. B **1**, 4784 (1970).
¹⁴For a pure metal at 4.2 K, the absorptivity in this region is described by the anomalous-skin-effect theory.
- While our calculated free-electron conductivity should not be assigned physical meaning, it does make it possible to see small interband effects which would otherwise be masked by the large free-electron conductivity.
¹⁵G. E. H. Reuter and E. H. Sondheimer, Proc. Roy. Soc. (London) **A195**, 336 (1948).
¹⁶T. Holstein, Phys. Rev. **88**, 1427 (1952); **96**, 525 (1954).
¹⁷R. Fuchs and K. L. Kliewer, Phys. Rev. B **2**, 2923 (1970).
¹⁸G. T. Meaden, *Electrical Resistance of Metals* (Plenum, New York, 1965).
¹⁹T. C. Cetas, J. C. Holste, and C. A. Swenson, Phys. Rev. **182**, 679 (1969).
²⁰P. B. Allen and M. L. Cohen, Phys. Rev. B **1**, 1329 (1970).

Enhancement of Sodium Self-Diffusion by Additions of Potassium[†]

J. N. Mundy and W. D. McFall

Argonne National Laboratory, Argonne, Illinois 60439

(Received 22 November 1971)

The diffusion coefficient of ²²Na has been measured in dilute potassium-sodium alloys (0–1.2 at. % potassium) at temperatures of 0 and 50 °C. Within experimental error a linear enhancement of the diffusion coefficient was observed at both temperatures. The data are analyzed in terms of different pairs of diffusion processes being responsible for the diffusion. While it is not possible to exclude other possibilities, the divacancy-vacancy explanation appears to be the most preferable.

I. INTRODUCTION

The unique determination of the mechanism of self-diffusion in a metal frequently requires the use of a number of different experimental techniques. The vacancy mechanism for diffusion in fcc metals was most clearly established by both measurements of thermal expansion and x-ray lattice parameter as a function of temperature and the isotope effect for self-diffusion. Further confirmation of the vacancy mechanism has come from measurements of the effect of pressure on self-diffusion, measurements of impurity diffusion, and the effect of solute additions to the self-diffusion coefficient. Although all these techniques, except that of influence of solutes, have been applied to sodium, it has not proved possible to uniquely establish the mechanism of diffusion. Indeed, recent measurements¹ show that more than one mechanism is operative in sodium and not one of these has been uniquely identified. The analysis of Neumann² of diffusion data in bcc metals indicates that sodium is not unusual and that the data for very few bcc metals truly justify the consideration of only one mechanism. The effect of potassium additions on the sodium self-diffusion coefficient have been

measured in an attempt to identify one or more of the diffusion mechanisms.

In most experimental studies, the variation of the self-diffusion coefficient with small solute addition (< 2%) is given by

$$D(c) = D(0) (1 + bc), \quad (1)$$

where c is the atomic fraction of the solute, and $D(c)$ and $D(0)$ are the diffusion coefficients of a solvent tracer in the alloy and pure solvent, respectively. Values of the enhancement factor b have been calculated for fcc metals in terms of three jump-frequency ratios by Lidiard³ and by Howard and Manning.⁴ The same three jump-frequency ratios are needed in the determination of the correlation factor for solute diffusion f_i and the ratio of solute to self-diffusion coefficient $D_i/D(0)$. The three experimentally measured quantities f_i , b , and $D_i/D(0)$ are interrelated by Eq. (1) and by the following equation given by Lidiard³:

$$f_i = 1 - \frac{4f_0}{b+18} \left(\frac{D_i}{D(0)} \right), \quad (2)$$

where f_0 is the correlation factor for the pure solvent. Measurements of these three quantities allows both a determination of the three jump-fre-